JOURNAL OF AGRICULTURAL AND FOOD CHEMISTRY

J. Agric. Food Chem. **2006,** *54,* 6835−6844 **6835**

Lipoxygenase Involvement in Ripening Strawberry

ANTONELLA LEONE,*,† TERESA BLEVE-ZACHEO,‡ CARMELA GERARDI,† MARIA T. MELILLO,‡ LUCIA LEO,† AND GIUSEPPE ZACHEO†

Consiglio Nazionale delle Ricerche, Istituto di Scienze delle Produzioni Alimentari, 73100 Lecce, Italy, and Consiglio Nazionale delle Ricerche, Istituto per la Protezione delle Piante, 70126 Bari, Italy

The enzymatic activity, subcellular localization, and immunolocalization of plant lipoxygenase (LOX) in strawberry fruits (*Fragaria* × *ananassa*, Duch) were investigated. Chemical and enzymatic properties of LOX have been characterized, and the LOX capability of oxygenating free and esterified unsaturated fatty acids into C_6 volatile aldehydes has been confirmed. Fruits at unripe, turning, and ripe stages were analyzed for LOX activity and protein localization by Western blots, two-dimensional electrophoresis, and immunolocalization analyses. The ability of strawberry tissues to in vivo metabolize linolenic acid or linoleic acid into C_6 volatile aldehydes and the LOX products was also analyzed. Analysis of strawberry proteins showed that a number of LOX forms, corresponding to at least two mobility groups of approximately 100 and 98 kDa and pI values ranging between 4.4 and 6.5, were present. Confocal and electron microscopy analyses support the idea that LOX proteins are associated to lipid−protein aggregates. Both exogenously supplied linoleate and linolenate were converted into hexanal and *trans*-2-hexenal at the three fruit-ripening stages. Our experiments suggest the presence of different LOX isoforms in strawberry fruits and that the lipoxygenase−hydroperoxide lyase pathway plays a role in converting lipids to C_6 volatiles during ripening.

KEYWORDS: Strawberry (*Fragaria* × *ananassa*, Duch); C_6 aldehydes; polyunsaturated fatty acids; lipoxygenase (LOX); hydroperoxide lyase (HPL); hydroperoxides (HPO)

INTRODUCTION

Lipoxygenases (LOXs; linoleate, oxygen oxidoreductase, E.C.1.13.11.12) are a family of nonheme, iron-containing dioxygenases, widely distributed in plants and animals. Several LOX isoforms have been identified in different cell compartments (*1*−*4*), and their activity has been associated to membranes of different origin, such as chloroplasts (*5*), lipid bodies (*6*), tonoplasts (*7*), and isolated plasma membranes (*8*). Chemical and enzymatic properties of plant LOXs have been extensively characterized, and it has been widely accepted that plant LOXs have various physiological roles in the plant metabolism (*2*). The presence of a number of LOX isoforms in the different subcellular compartments makes it difficult to assign a specific function to each LOX isoform. Some evidence suggests that LOXs are correlated with certain processes: growth regulation, maturation, senescence, and wound- and pathogen-induced defense (*9*−*12*).

Plant LOXs catalyze the dioxygenation of 1,4 pentadiene cis-polyunsaturated fatty acids into their corresponding hydroperoxide derivatives (HPO), highly reactive compounds, which can be further metabolized by other enzymes of the so-called LOX pathway [allene oxide synthase, hydroperoxide lyase (HPL), peroxygenase, or divinyl ether synthase] into a cascade of bioactive products (*2*). The oxidation of lipids, by the sequential action of LOX and HPL, is reported to produce volatile compounds, which contribute to flavor and aroma in many plant tissues (*13*−*16*). Distinct plant LOX isozymes preferentially incorporate oxygen into either the C-9 or the C-13 position of linoleic (LA) and linolenic acids (LNA) to produce 9-(*S*)- or 13-(*S*)-hydroperoxy octadecadienoic acid (HPOD) or 9-(*S*)- or 13-(*S*)-hydroperoxy octadecatrienoic acid (HPOT), respectively. Both 9- and 13-hydroperoxides can subsequently be cleaved to C_{12} or C_9 ω-oxo-fatty-acids and volatile C_6 and C_9 aldehydes, respectively, by the action of HPL enzymes, recently characterized as a special class of cytochrome P450 (*17*). Volatile aliphatic C_6 compounds are important constituents of characteristic fruit flavors and aromas, especially of the "fresh green" aroma. The involvement of the LOX pathway in the biosynthesis of fruit aroma compounds has been reported in tomato (*18*, *19*), olive (*15*), bell pepper (*20*), apple (*14*), citrus (*21*), and strawberry (*13*). The function of LOXs and HPL in fruit ripening is not known, but their involvement in strawberry ripening has been suggested (*13*).

The development of aroma in strawberry fruits is a very complex process involving a large number of volatile molecules such as esters, saturated and unsaturated aldehydes and alcohols, sulfur compounds, and furanone-derived compounds (*22*, *23*). The components of strawberry aroma are well-known (*24*), and

* To whom correspondence should be addressed. Tel: +39 0832 422615. Fax: +39 0832 422620. E-mail: antonella.leone@ispa.cnr.it.
† Istituto di Scienze delle Produzioni Alimentari.
‡ Istituto per la Protezione delle Piante.

10.1021/jf061457g CCC: $33.50
Published on Web 08/08/2006

a better understanding of the processes underlying strawberry fruit maturation was recently reached through DNA microarray technology (*25*). However, valuable information about biochemical and molecular events, which control strawberry fruit development and ripening, is still lacking. Some evidence suggests that fruit ripening is related to senescence processes involving membrane lipid metabolism (*26*). Thompson et al. (*26*) supported the hypothesis of the role of LOX in the loss of membrane integrity associated with senescence in plants. In particular, the finding that lipid−protein particles in Carnation petals are enriched in LOX pathway-derived C_6 aldehydes and alcohols (*27*) points to the fact that lipid-metabolizing enzymes are involved in aroma component biosynthesis.

In view of the above hypotheses and considering that C_6 volatile compounds are derived from polyunsaturated fatty acids via the LOX pathway (*2*, *11*), the aim of this study is to answer the question as to whether strawberry LOX is associated with lipid peroxidation and the development of flavor in strawberry fruits. A histochemical, biochemical, and physiological approach to elucidate the subcellular localization of LOXs and the functional role of these proteins in strawberry tissue is here reported. The changes in LOX and HPL activities and their relationship in the biosynthesis of volatile products in strawberry fruits during ripening are also discussed.

EXPERIMENTAL PROCEDURES

Plant Material. Strawberry plants (*Fragaria* × *ananassa*, Duch, cv. Paros) were grown in a greenhouse, and the fruits were harvested at three ripening stages: unripe, turning, and ripe stages (corresponding approximately to 10, 24, and 30 days from anthesis, respectively). Fresh fruits were immediately analyzed for C_6 volatile biosynthesis, embedded for microscopy studies, or cut into four pieces, frozen in liquid nitrogen, and stored at −40 °C for further experiments.

Enzyme Extractions and Enzymatic Assays. LOXs were extracted from strawberry fruits at unripe, turning, and ripe stages in 0.1 M Tris-HCl, pH 8.0 (buffer A). The same buffer with 0.1% Triton X-100 added (buffer B) was used to extract the HPL enzymes. Ten grams of frozen strawberries at the different ripening stages was homogenized in a Waring blender with 2 g of PVPP (polyvinylpolypyrrolidone, Sigma) and 20 mL of extraction buffer (A or B) containing 1 mg/mL of Protease Inhibitor Cocktail (Sigma). For crude extract preparation, the homogenate was filtered through two layers of Miracloth (Calbiochem-Novachem Co., La Jolla, CA) and centrifuged for 20 min at 1000*g* at 4 °C to remove cell debris. For the biochemical localization of LOX activity, a subcellular fractionation was performed. The homogenate, obtained as described above, was centrifuged at 10000*g* for 20 min at 4 °C; the upper fraction of the supernatant was transferred, diluted with the same extraction buffer, and centrifuged at 15000*g* for 10 min at 4 °C. The upper layer, corresponding to the crude lipid body-enriched fraction (LBF), was collected, refloted twice, and analyzed. After the lipid layer had been removed from the 10000*g* supernatant, the remaining supernatant was ultracentrifuged at 150000*g* for 120 min at 4 °C and the resulting supernatant was the soluble fraction (SF). The pellet was washed with buffer A, suspended in buffer A together with 1 mM KCl, and centrifuged at 20000*g* to remove undissolved material. The supernatant was used as the microsome-enriched fraction (MF). Proteins were quantified by the dye-binding method of Bradford (*28*) using bovine serum albumin (BSA, Sigma) as standard.

LOX Assay. The LOX activity was spectrophotometrically determined by measuring the formation of conjugated dienes at 234 nm and 25 °C (*29*). The reaction was also performed in presence of 1 mM KCN to verify if the enzymatic activity was cyanide-resistant (*33*). Linoleic acid (LA), LNA, linolenic acid methyl ester (MLNA), linoleic acid methyl ester (MLA), trilinolein (TLA), and trilinolenin (TLNA) (Sigma) were used as substrates to evaluate the specific activity of LOX. The activity (expressed as nmol of hydroperoxide formed min^{-1} mg^{-1} of proteins) was calculated by measuring the changes in absorbance at 234 nm using a molar extinction coefficient of 25000 M^{-1} cm^{-1}. In order to determine the optimum pH of the reaction, assays of LOX activity were carried out using different buffers, buffer I (0.1 M Na-acetate at pH 4.0, 4.5, 5.0, and 5.5, respectively), buffer II (0.1 M Na-phosphate at pH 6.0, 6.5, 7.0, and 7.5, respectively), and buffer III (50 mM Tris-HCl at pH 8.0, 8.5, 9.0, and 9.5, respectively), and LA and LNA as substrates.

Identification of LOX Products. Crude extracts from strawberry at the three different ripening stages were incubated for 30 min in 1 mL of 0.1 M Na-phosphate buffer, pH 6.0, containing either 0.3 mM LA or LNA. Reaction products were reduced with sodium borohydride, extracted with chloroform/methanol (2:1, v/v), and dried. The reaction products were suspended in methanol/water/acetic acid (85:15:0.1, v/v/v) and separated by reverse phase high-performance liquid chromatography (RP-HPLC) using a C18 Ultrasphere column (Beckmann, 0.46 cm × 25 cm) as already reported (*30*). The peak adsorbing at 234 nm containing either hydroxy octadecadienoic acid (HODE) or hydroxy octadecatrienoic (HOTE) isomers was collected, dried, and suspended in *n*-hexane/propan-2-ol/acetic acid (100:2:0.1, v/v/v). The 9-HODE and 13-HODE were separated by straight-phase (SP) HPLC with a Silica Ultrasphere column (Beckmann, 0.46 cm × 25 cm) as already described (*30*). Authentic standards of 9- and 13-HODE were purchased from ICN. HPLC analyses were carried out using a Beckman System Gold apparatus (Beckman Coulter, Inc.) equipped with a 126 solvent module and a 168 detector.

HPL Assay. The HPL activity was analyzed by evaluating the hexanal production using headspace gas chromatography−mass spectrometry (HS-GC-MS). The reaction mixture (1 mL) contained 0.1 M Na-phosphate buffers, pH 6.0, 50 μM 13-hydroperoxy-linoleic acid (13-HPODE, Sigma), or 50 μM 9-hydroperoxy-linolenic acid (9-HPOTE, Larodan, Malmö, Sweden) and 100 μL of crude extract. The reaction mixtures and the appropriate controls without substrate or without enzyme were incubated at 25 °C for 15 min in a 10 mL sealed vial. The reaction was stopped by adding 12 N HCl until the solution reached pH 3. The vials were then transferred into an automatic HS sampler (Shimadzu AOC-5000) and analyzed by HS-GC-MS. A 10 min equilibration time at 120 °C was set to develop volatile compounds. These volatile components were analyzed using a Shimadzu GC 17-A gas chromatograph equipped with a Shimadzu QP 5050 mass spectrometer. GC analysis was performed using helium as a gas carrier on 30 m × 0.25 mm i.d. Alltech Econo-Cap EC^{TM-5} capillary column at programmed temperatures ranging from 40 to 230 °C at 4 °C/min. Mass spectrometer parameters were as follows: 250 °C, injection temperature; 230 °C, interface temperature; 70 eV, ionization voltage; and 50−400 *m*/*z*, mass range. Volatile components were identified by comparison of the obtained mass spectra to the NIST mass spectrum library and to the spectra of standards. The amounts of hexanal and *trans*-2-hexenal were calculated by a calibration curve with standards (Sigma) in the range 10−1000 nmol by GC-MS Postrun Analysis software (Shimadzu, Co.). HPL activity was expressed as nmol of hexanal formed min^{-1} mg^{-1} of protein.

Lipid Hydroperoxide Assay. Fresh strawberry fruit tissues at the three ripening stages were ground in liquid N_2 and homogenized in 5 volumes of 100% ethanol and centrifuged at 1000*g* for 10 min at 4 °C, and the supernatant was assayed for HPO content. The whole procedure was directed to minimizing enzymatic and nonenzymatic HPO content modification. HPO levels were measured spectrophotometrically with the Xylenol Orange technique. The Xylenol Orange reagent (2 mL) was added to the sample (50−100 μL), and the volume was adjusted to 2.1 mL with ethanol (*31*). The mixture was incubated at room temperature for 45 min, and the absorbance at 560 nm was measured against a blank mixture of 2 mL of Xylenol Orange and 100 μL of ethanol. Fresh solutions of cumene hydroperoxide were used for the construction of the dye calibration curve.

In Vivo Conversion of LA and LNA into C_6 Volatile Aldehydes. Fruits at unripe, turning, and ripe stages were harvested from plants grown under controlled conditions and immediately transferred into 20 mL vials containing either 5 mL of 0.1 M Na-phosphate buffer, pH 6.0, (control) or the same buffer with 0.3 mM LNA or LA, added as substrate and dissolved as described in Axelrod et al. (*29*). Five grams from the whole fruits was submerged in the reaction mixture (with or without substrate) and quickly and thickly sliced (2−3 mm). The vials

were sealed immediately, vigorously agitated for 5 s, and maintained at 25 °C for 10 min before HS-GC-MS analysis. Vials containing only the reaction mixture were used as a blank. The amount of hexanal and *trans*-2-hexenal was calculated by calibration curves with standards (Sigma) in the range of 1−1000 nmol by GC-MS Postrun Analysis software (Shimadzu, Co.). The biosynthesis by the LOX-HPL pathway was evaluated as hexanal and *trans*-2-hexenal formed min^{-1} g^{-1} of fresh weight as compared with the control value obtained using sliced fruits in the buffer (0.1 M Na-phosphate buffer, pH 6.0) without substrates.

Sodium Dodecyl Sulfate (SDS)-Polyacrylamide Gel Electrophoresis (PAGE) and Western Blotting. Proteins, extracted as described above, were diluted with SDS-PAGE sample buffer, and the final buffer concentration was 0.0625 M Tris-HCl buffer (pH 6.8) containing 2.3% (w/v) SDS, 10% (v/v) glycerol, 5.0% β-mercaptoethanol, and 0.01% (w/v) Bromophenol Blue. Samples were heated at 95 °C for 5 min and separated on 15% SDS-PAGE. An equal amount of proteins for each sample was loaded on gels. Bio Rad broad molecular weight markers were used as standards. After electrophoresis, gels were blotted on nitrocellulose membrane Hybond C extra (Amersham) and polypeptides were probed with polyclonal antibodies obtained against LOX proteins from cucumber cotyledons (*32*). LOX IgG bounded proteins were detected using anti-rabbit IgG-Perox linked in donkey (Amersham, Bioscience) and revealed by the ECL detection method (Amersham). Marker proteins on blots, stained with 0.5% (w/v) Ponceau S (Sigma) in 5% (v/v) trichloracetic acid (TCA), were used to determine the apparent relative molecular mass (M_r) of proteins. Membranes were incubated either with antibody anti-LOX or with secondary antibody only as controls.

Bidimensional Electrophoresis (2DE). Strawberry fruits were homogenized in liquid nitrogen using a Waring blender. Samples were extracted by incubation for 1 h at room temperature in Laemmli buffer containing 65 mM dithiothreitol (DTT, Sigma), 2% PVPP, and a protease inhibitor cocktail (Sigma). The extracts were centrifuged for 10 min at 12000*g* at 4 °C, and the supernatants were incubated for 10 min at 95 °C. The extracts were then centrifuged for 30 min at 60000*g* at 4 °C. Proteins were then precipitated using the Clean-Up kit (Amersham Biosciences) and suspended in Rabilloud buffer containing 7 M urea (Sigma), 2 M thiourea (Sigma), 4% CHAPS (Sigma), 1% DTT, and 20 mM Tris. Samples (300 μL) were electrofocused in a Bio-Rad Protean IEF cell using IPG Ready strips (17 cm, range of pH 4−7) at about 80 kVh. SDS-PAGE was performed using 8−16% precast gels (Bio-Rad). After electrophoresis, proteins were visualized by Brilliant Blue G colloidal (Sigma-Aldrich, Inc.) or gels were electroblotted on nitrocellulose membranes for immunodetection with anti-LOX antibodies.

Tissue Printing. Tissue printing and immunolocalization were performed as described by Kausch and Handa (*18*) with some modifications. Strawberry receptacles at the three stages of ripening were separated longitudinally along their sagittal section into two halves with a razor blade. Sections were placed for 1 min on chromatography paper Whatman 3 MM saturated with 0.1 M Na-phosphate (pH 6.5). The samples were briefly dried with Whatman paper and placed on nitrocellulose membranes Hybond C extra (Amersham) for 10 min. Tissue prints were washed in bidistilled water, stained for total proteins with Ponceau S reagent (0.5% w/v in TCA 5% v/v) for 5 min, and destained with repeated changes of bidistilled water. Blots were processed as described in the SDS-PAGE and Western blotting section. Opportune controls without either primary or secondary antibodies were conducted.

Immunolocalization by Confocal and Electron Microscopy. Strawberry tissues at the three stages of ripening were cut into pieces approximately 3−4 mm diameter and fixed and embedded as reported in Leone et al. (*33*). Thick sections collected on poly-L-lysine (Sigma)-coated slides were treated with aqueous 0.56 M sodium periodate for 1 h at room temperature, thoroughly rinsed with bidistilled water, and then treated with 0.1 M HCl. After 30 min, the sections were washed at least twice with water and permeabilized with 1% Triton X-10 and 0.1% BSA in PBS (10 mM phosphate buffer, 150 mM NaCl) for 30 min. The slides were treated with 1:10 preimmune goat serum (Amersham) in PBS−BSA for 1 h. After they were washed in PBS−BSA, the sections were incubated either with anti-LOX antibodies in PBS−BSA (1:50) or with preimmune serum for 1 h. Sections then were washed and incubated with goat anti-rabbit immunoglobulins conjugated with AlexaFluor 633 (Molecular Probes, Inc., Eugene, OR) in PBS−BSA (1:50) for 1 h in the dark. Different sections incubated (i) with primary antiserum alone, (ii) with primary antibody, or (iii) with secondary antibody were used as controls. An excess of antibody was removed by repeated washing either with PBS−BSA or PBS buffer for 10 min. The slides were covered with a coverslip and examined under a dual-channel laser confocal system (LSM Pascal, Zeiss) coupled to an Axiovert 200 inverted microscope (Zeiss) and equipped with He-Ne and Ar lasers. The 633 nm line of the He-Ne laser was used to excite AlexaFluor-633 labeled tissues, and the 488 nm Argon line was used to excite autofluorescence. Manufacturer-supplied LSM 5 Pascal software version 2.8 was used to control image acquisition.

For the immuno-gold labeling, thin sections from the samples used for the immunofluorescent assay were treated as described in Leone et al. (*33*). Ultrathin sections treated with 1:100 anti-LOX antibody and 1:20 secondary anti-rabbit antibody 10 nm gold conjugated (Auroprobe EM GAR G10, Amersham) were stained with 2% aqueous uranyl acetate and 1% lead citrate and observed under a Philips 400T electron microscope.

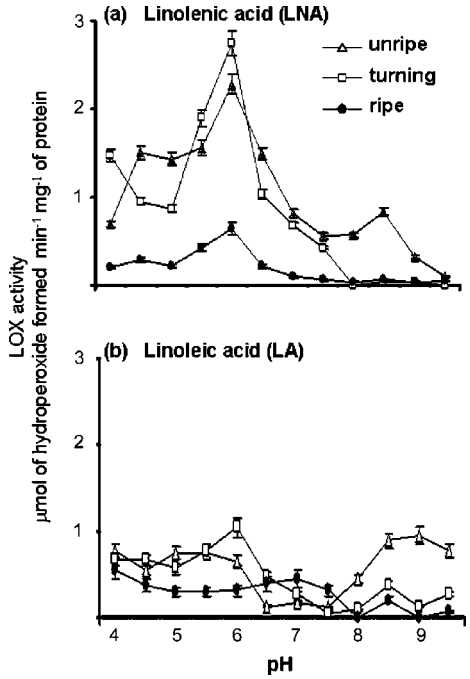

Figure 1. Effect of pH on LOX activity in strawberry fruit extracts at unripe (triangles), turning (boxes), and ripe (circles) stages. The LOX activity was assayed at different pH values using three different buffers (buffer I, 0.1 M Na-acetate at pH 4.0, 4.5, 5.0, and 5.5; buffer II, 0.1 M Na-phosphate at pH 6.0, 6.5, 7.0, and 7.5; and buffer III, 50 mM Tris-HCl at pH 8.0, 8.5, and 9.0) and using (**a**) LNA and (**b**) LA as substrates. Data are means ± standard errors from three independent experiments.

RESULTS

Characterization of Strawberry LOX Activity. To investigate the behavior of LOXs during strawberry ripening, the LOX activity was spectrophotometrically measured and the concentrations of the obtained hydroperoxides were plotted against the pH (**Figure 1**). The specific activity of LOX, at the considered pH range (4.0−9.5), was higher with LNA than with LA, in both unripe and turning fruits, while no significant differences were detected in the ripe strawberry (**Figure 1a**,**b**). A sharp peak of LOX activity occurred in extracts of the unripe and turning stages incubated in 0.1 M Na-phosphate buffer at pH 6.0 with LNA as the substrate; only a small peak in ripe

Table 1. LOX Activity in Strawberry Extracts at the Three Different Stages of Ripening, Using Different Substrates

	LOX activity (nmol of hydroperoxide formed min^{-1} mg^{-1} of protein)[a]		
	stage of ripening		
substrates	unripe	turning	ripe
LNA	2279 ± 115	2743 ± 137	640 ± 33
LA	662 ± 42	1041 ± 55	320 ± 21
MLNA	519 ± 25	1171 ± 58	407 ± 18
MLA	679 ± 33	1869 ± 98	702 ± 25
TLNA	2725 ± 299	2430 ± 220	2017 ± 231
TLA	990 ± 55	436 ± 53	380 ± 21

[a] Data are means ± standard errors from six independent experiments.

strawberry at the same pH was observed. Analysis of LOX activity in the presence of LNA revealed small peaks at basic pH only in the unripe fruit extracts. At acidic pH, additional peaks were detectable in unripe and turning fruits (**Figure 1a**). When the LOX activity was measured in the presence of LA in the unripe fruit extracts, two minor peaks were observed at neutral and basic pH, while in turning fruits a single peak at neutral pH was noticed. In ripe fruits, the LOX activity was low in all ranges of the pH (**Figure 1b**). As the maximum of enzyme activity was detected in 0.1 M Na-phosphate buffer at pH 6.0 in all of the ripening stages, this buffer was used to measure LOX activity in subsequent experiments.

In addition to free fatty acids (linoleate and linolenate), strawberry LOXs exhibited the ability to exploit esterified unsaturated fatty acids (methyl linoleate, methyl linolenate, TLA, and TLNA) at the three stages of ripening (**Table 1**). LOX enzymes exhibited higher affinity for TLNA and LNA than for LA, methyl linoleate, methyl linolenate, and TLA. The highest specific LOX activity, with most of the used substrates, was observed at the turning stage, the lowest in the mature strawberry. The LOX activity gradually decreased during ripening when TLA and TLNA were used as substrates (**Table 1**). When the activity was calculated as activity per amount of protein present in 1 g of fresh weight tissue, the total LOX activity resulted much higher at the turning stage than at the other two stages. Although in ripe fruits the amount of protein per gram of fresh weight was higher than in both unripe and turning fruits, less total LOX activity was found.

HPO Amount and LOX Product Specificity. The HPOs were detected in the fruit tissues at all of the ripening stages although slightly less in the turning and ripe stages (**Figure 2a**). In order to characterize the LOX(s) of ripening strawberry as 9- and/or 13-LOX, the LOX reaction products, using LA or LNA as substrates, were analyzed by RP-HPLC. The LOX reaction products were reduced with sodium borohydride and separated by RP-HPLC. The peak adsorbing at 234 nm, containing the hydroperoxides, was collected and subjected to SP-HPLC to separate 13- and 9-HODE (13- and 9-HOTE). The retention times of the products obtained from the strawberry LOX reaction were compared with the reaction products of soybean LOX type I (13-LOX) and 9- and 13-HODE standards. The products of the strawberry LOX reaction were both 9- and 13-HODE at all considered stages. The rate between the two isomers was about 3:7 (13-HODE/9-HODE) at unripe and turning stages and about 1:1 at the ripe stage (**Figure 2c**). Similar results were obtained using LNA as the substrate (data not shown). The results indicate that the amounts of the detected HPO comprise the LOX reaction products. In addition, both 9- and 13-LOX are present at all ripening stages, and it is

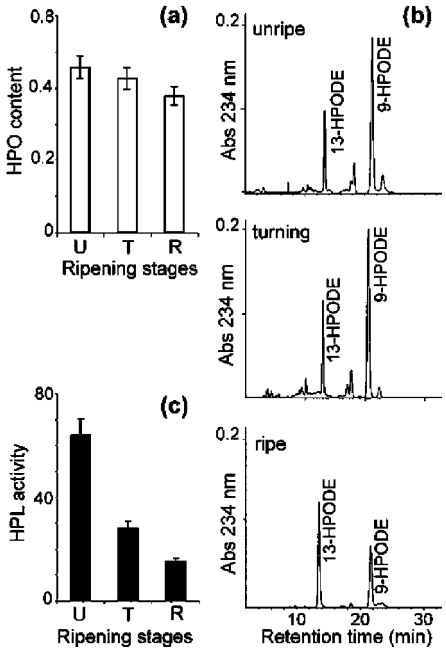

Figure 2. Analysis of LOX- and HPL-derived products in unripe (U), turning (T), and ripe (R) in strawberry fruits. (**a**) Lipid HPO content in strawberry tissues expressed as μmol of HPO g^{-1} of fresh weight (HPO content). (**b**) HPLC analysis of hydroxyl-fatty acids produced by strawberry LOX expressed as absorbance at 234 nm (Abs 234 nm). One hundred micrograms of total proteins from unripe, turning, and ripe strawberry was incubated for 30 min in 0.1 M sodium phosphate buffer, pH 6.5, containing 0.3 mM LA. Reaction products were first separated by RP-HPLC and then by SP-HPLC as described in the Experimental Procedures. (**c**) HPL activity measured as hexanal formation after incubation of strawberry protein extracts in the presence of 13-HPOD and expressed as nmol of hexanal-formed min^{-1} mg^{-1} of proteins. Data are means ± standard errors from three independent experiments.

interesting to note a major 9-LOX activity at the early ripening stages. This suggests the presence of a changing pool of LOX enzymes in strawberry crude extract.

In Vitro HPL Activity. To assess the putative role of LOXs in strawberry and to relate their activity to the development of some volatile compounds catalyzed by the enzymes of the LOX-HPL pathway, the in vitro HPL activity and in vivo production of C_6 volatile aldehydes were evaluated. The maximum HPL activity, measured as volatile products formed in the presence of 13-HPOD, occurred in extracts from green fruits and decreased quickly during ripening (**Figure 2c**). 9-HPOT resulted also as a good substrate for strawberry HPL giving rise to the volatile aldehyde, nonadienal (data not reported). No volatile aldehyde production was detected in the absence of 9-HPOT, 13-HPOD, or enzyme extracts.

In Vivo Conversion of LA and LNA into C_6 Volatile Aldehydes. To evaluate whether strawberry tissues are able to metabolize LNA (the typical precursor of *trans*-2-hexenal in plants) or LA (precursor of hexanal) into C_6 volatile aldehydes through the LOX-HPL pathway in vivo, the amounts of *trans*-2-hexenal and hexanal formed in the presence of either LA or LNA were analyzed by HS-GC-MS (data were compared with those obtained in the absence of exogenous substrate). The endogenous hexanal was present at all ripening stages and increased during ripening. The endogenous *trans*-2-hexenal was detectable in traces in unripe fruits and increased during ripening (**Table 2**). These C_6 aldehydes could have a different HS-GC-MS detection threshold, due to their different polarity and to a

Table 2. Conversion of LNA and LNA into C_6 Volatile Aldehydes in Ripening Strawberry Fruits at Unripe, Turning, and Ripe Stages[a]

ripening stages	C_6 aldehydes types	formation of C_6 volatile aldehydes (pmol min^{-1} g^{-1} of fresh weight)[b]		
		buffer	LA	LNA
unripe	hexanal	125 ± 35	2646 ± 99	257 ± 25
	trans-2-hexenal	0.5 ± 0.3	ND[c]	4 ± 0.8
turning	hexanal	325 ± 60	1398 ± 27	1118 ± 14
	trans-2-hexenal	5 ± 0.5	2 ± 0.5	59 ± 3
ripe	hexanal	1298 ± 53	2604 ± 49	1155 ± 83
	trans-2-hexenal	14 ± 2	51 ± 9	85 ± 10

[a] Five grams of fruits of each stage was kept in vials with 5 mL of 0.1 M Na-phosphate buffer, pH 6.0 (control), or in the same buffer containing 0.3 mM LA or LNA, respectively, as substrates. The reaction was performed for 10 min, at 25 °C, in sealed vials, before HS-GCMS analysis. The hexanal and *trans*-2-hexenal formation were expressed as pmol of C_6 volatile aldehydes formed min^{-1} g^{-1} of fresh weight. [b] Data are means ± standard errors from three independent experiments. [c] Not detected.

different entry into the HS. This could explain why the amount of *trans*-2-hexenal detected was much lower than that of the hexanal. Anyway, both exogenously supplied linoleate and linolenate were metabolized into hexanal and *trans*-2-hexenal by the fruit at the three ripening stages (**Table 2**). In the presence of exogenous LA, the hexanal production was enhanced and the increased hexanal resulted higher in unripe than in either turning or ripe tissues. An increased amount of *trans*-2-hexanal in ripe fruits was also observed. In the presence of LNA, the levels of *trans*-2-hexenal increased during the ripening process; hexanal increased at the unripe and the turning stages. The presence of de novo formed hexanal, in the presence of exogenous LNA and *trans*-2-hexenal in the presence of LA, suggested that the transformation of *trans*-2-hexenal to hexanal and vice versa can occur. As compared to mature fruits, unripe strawberry displayed a different metabolism for the two polyunsaturated fatty acids. The biosynthesis of hexanal was most significant in unripe strawberry, shifting to *trans*-2-hexanal formation in the mature fruit. In addition, the occurrence of C_6 alcohols and ethyl hesanoate in the presence of LNA (data not shown) indicated that some of the LOX-HPL pathway products were transformed into alcohols and acids and promptly esterified by unspecific acyltransferase present in ripe fruits, consistent with Aharoni et al. (*25*).

Localization of LOX Activity. In order to establish whether other LOX isoforms were involved in strawberry fruit ripening, the LOX activity was analyzed in different subcellular compartments. The LOX specific activity, assayed in the presence of various substrates, was detected in all of the isolated fractions: LBF, SF, and MF (**Table 3**). The data proved that LOX activity was higher in MF than in the other fractions, when analyzed in the presence of LA and LNA while LOX activity in LBF fractions was remarkably high in the presence of esterified fatty acids. The LOX activity assayed with LA and LNA decreased in the SFs and LBFs during ripening, it slightly increased in the MF at the turning stage, and it dropped in mature fruits. As a rule, the enriched lipid body fraction showed a higher LOX activity in the presence of TLA and TLNA than in the presence of LA and LNA. The LBF LOX activity, assayed with esterified fatty acids, was high in the unripe and turning stages and decreased in the ripe stage. An increased LOX activity during ripening was detected in the soluble fraction when TLNA was used as a substrate. However, no significant differences in LOX activity were detected in the presence of TLA. The LOX activity in microsome-enriched fractions at both unripe and turning stages was similar or higher in the presence of LA and LNA than in the presence of their analogous esterified fatty acids. At the ripe stage, LOXs showed a similar activity with all of the substrates used, except for TLNA.

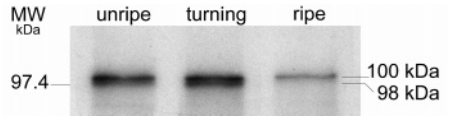

Figure 3. Western blot analysis of LOX protein from strawberry tissue extracts. Equivalent amount of total proteins extracted from unripe, turning, and ripe fruits were separated by SDS-PAGE, blotted to nitrocellulose membranes, and probed with anti-LOX antibodies. MW, molecular weight standard: 97.4 kDa (phosphorilase B).

Western Blots Analyses. In order to identify LOX proteins in strawberry fruit extracts, monodimensional electrophoresis and 2DE and Western blot analyses were performed. The changes in the profile of LOX proteins in unripe, turning, and fully mature fruits as shown by SDS-PAGE and Western blot analysis are reported in **Figure 3**. The anti-LOX antibodies recognized a polypeptide of approximately 100 kDa in the total protein extracts from fruits at all three ripening stages. A weak second band of approximately 98 kDa was also detected at the unripe and the turning stages. The 100 kDa polypeptide increased at the turning stage and decreased in ripe fruits, while the 98 kDa polypeptide was clearly visible at both unripe and turning stages and was not detectable in ripe fruits. The immunoreaction was higher in protein extracts from the unripe and turning stages than from those at the ripe stage.

To further explore the changes of LOX during ripening, Western blot analysis of the 2DE of the total proteins was performed (**Figure 4**). A comparison of the LOX immunoreactive spots present in the 2DE protein maps of strawberry fruits at the unripe, turning, and ripe stages showed that a definite number of spots were detectable at the various ripening stages and that there were some stage-specific spots (circled). Spot

Table 3. LOX Activity in LBF, SF, and MFs from Strawberry at Three Different Ripening Stages: Unripe, Turning, and Ripe[a]

	LOX activity (nmol of hydroperoxide formed min^{-1} mg^{-1} of protein)[b]								
	stage of ripening								
	unripe			turning			ripe		
substrates	LBF	SF	MF	LBF	SF	MF	LBF	SF	MF
LNA	335 ± 52	1516 ± 89	2311 ± 102	84 ± 14	856 ± 23	2404 ± 98	15 ± 5	158 ± 21	493 ± 38
LA	568 ± 65	1701 ± 47	1163 ± 67	194 ± 22	991 ± 32	1792 ± 44	123 ± 12	155 ± 12	291 ± 35
TLNA	8900 ± 243	1350 ± 99	2534 ± 145	9129 ± 112	1414 ± 45	794 ± 53	3420 ± 122	5362 ± 132	717 ± 65
TLA	3505 ± 67	972 ± 45	1797 ± 54	3081 ± 87	1064 ± 72	595 ± 45	740 ± 58	619 ± 99	408 ± 41

[a] LOX activity was measured as nmol of hydroperoxides formed min^{-1} mg^{-1} of proteins with free fatty acids, linoleate and linolenate, and with esterified fatty acids, TLA and TLNA, as substrates. [b] Data are means ± standard errors from three independent experiments.

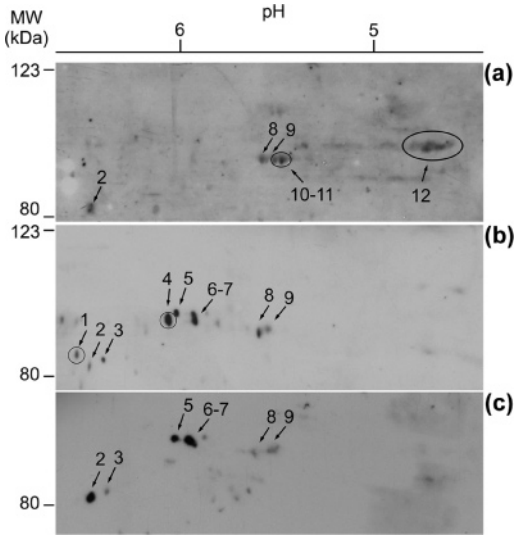

Figure 4. Western blot analysis of 2DE separation of proteins from strawberry tissues. Total proteins extracted from (**a**) unripe (0.036 mg of proteins), (**b**) turning (0.48 mg of proteins), and (**c**) ripe (0.69 mg of proteins) fruits were fractionated by 2DE, blotted on nitrocellulose membranes, and probed with anti-LOX antibodies. MW, molecular weight standard: 123 (β-galalctosidase) and 80 kDa (BSA). Number-arrow indicates immunoreactive spots; circled spots indicate stage-specific immunoreactive spots.

numbers 1 and 4 were stage specific to the turning stage while spot numbers 10 and 11 and the polypeptides at pI 4.5−4.7, indicated as number 12, were visible only at the unripe stage. As can be seen in **Figure 4**, at the unripe stage, the anti-LOX antibodies mainly recognized one train of spots of approximately 100 kDa, with a pI ranging from pH 5.4 to pH 5.6 (spot numbers 8−11), and a second train (number 12), with a molecular weight slightly higher than 100 kDa and a pI ranging between 4.5 and 4.7. The spot numbers 2, 8, and 9 (pI 6.4, 5.6, and 5.4, respectively) were observed at all ripening stages (**Figure 4a**−**c**). In the turning strawberry fruits (**Figure 4b**), the immunoreactive polypeptide pattern showed a marked change: Spot number 12 was not detectable, while some spots with similar molecular masses and neutral pI values appeared (spot numbers 4−7, which had pI values of 6.1, 6.0, 5.95, and 5.9, respectively). Moreover, at the turning stage, three spots (numbers 1−3) with a molecular mass of around 80 kDa, characterized by pI values of 6.5, 6.4, and 6.3, were present. Spot number 1 was only detected in turning fruits while spot number 3 was present at the turning and the ripe stages but not at the unripe stage.

Immunochemical Localization of LOX Proteins in the Tissues. In order to clarify the features of strawberry LOXs, LOX proteins were analyzed in strawberry fruit tissues by means of tissue printing and immunocytochemical techniques.

Tissue Printing. Tissue printing experiments to localize LOX proteins at tissue level showed that sagittal sections of the receptacle at different stages of ripening (**Figure 5a**) were immunodecorated by anti-LOX antibodies when printed on nitrocellulose membranes (**Figure 5b**). On the basis of the observations that the immunoreactive proteins were mainly located in the outer cortical region of the receptacle at all three ripening stages (**Figure 5b**$_1$−**b**$_3$), 3−5 mm of subepidermal cortical tissue was selected for immunolocalization by confocal and electron microscopy.

Confocal Microscopy Analysis. Immunofluorescence confocal laser scanning microscopy (CSLM) studies were performed to localize LOX proteins within the receptacle tissues of strawberry fruits at the three ripening stages. The distribution of LOX proteins at the subcellular level was analyzed in the parenchyma cells. When challenged with anti-LOX antibodies, the LOX protein in the sagittal sections of the fruit was indirectly visualized by red fluorescence of Alexa Fluor 633 conjugated with secondary antibody (**Figure 5**). Immunolabeled sections of the cortical region of the strawberry fruits were examined, and optical sections and their projections were generated by CLSM software. The histological features of parenchyma cells and vascular tissues were visualized at 488 nm laser line, which excited autofluorescence (green virtual color). The parenchyma cells of the receptacle exhibited red fluorescence upon immunoreaction, indicating the presence of LOX proteins (**Figure 5e**−**g**). No red fluorescent label but only plant tissue autofluorescence (green) was detectable in the control fruits incubated with preimmune serum (**Figure 5d**). Confocal images of unripe (**Figure 5e**), turning (**Figure 5f**), and ripe (**Figure 5g**) fruits showed that LOX proteins localized differently during the ripening process. LOX proteins were evidenced in the parenchyma cells of the receptacle, especially in the subepidermal cell layers and in those parenchyma cells close to the vascular bundles. **Figure 5c** shows the cortex of an unripe receptacle formed by a single layer of epidermal cells and a subepidermal parenchyma with isodiametric to slightly radially elongated, thin-walled cells. Strong red labeling on the endomembrane system and the lipid−proteinlike globular bodies were detected close to the walls of the subepidermal parenchyma cells (**Figure 5e**). Fluorescent globular bodies occupied the most part of several unripe receptacle parenchyma cells. During ripening, large and loosely packed parenchyma cells formed the bulk of the cortex in the receptacle. Labeled globular bodies were reduced in size and compressed between the vacuoles and the walls, the lumen of these cells being 95% occupied by a central vacuole (**Figure 5f**). In ripe receptacle parenchyma, where vacuoles occupied the majority of the cell and the cytoplasm was reduced to the cell periphery, only a red-labeled strip lying along the cell wall was detectable (**Figure 5g**).

Electron Microscopy Analysis. The occurrence of LOXs at subcellular level, receptacle parenchyma tissue, was analyzed by electron microscopy. Micrographs of LOX immunolocalization seem to support the confocal microscopy observations (**Figure 6**). The structure of parenchyma cells in unripe fruit revealed that apart from the cell wall, nucleus with nucleoli, and chloroplasts, a complex system of membranes was also present (**Figure 6a**). Electron-dense structures, round in shape and with a dense core, were also detected. At higher resolution, these structures were seen to be irregular aggregates of electron-dense material (presumably lipid−protein aggregates) (**Figure 6b**,**c**). Gold particles associated to LOX proteins were detected in the cytoplasm, mainly enriching the profiles of some membranous structures (probably ER) and the outer part of the lipid−protein aggregates (**Figure 6b**,**c**,**e**). The electron-dense core resulted as unlabeled (**Figures 5c** and **6b**,**e**). Cell walls, nuclei, nucleoli, plastids, and mitochondria appeared essentially free of labeling or showed rare scattered gold particles at a very low level similar to that of the control where anti-LOX antibodies were omitted (**Figure 6d**). During fruit ripening, the lipid−protein structures seemed to coalesce into larger and more homogenously electron-dense aggregates than at the unripe stage. Gold particles, at the ripe stage, were only detectable scattered in the cytoplasm of parenchyma cells, in the disaggregating endomembrane system and on the surface of lipid aggregates (not shown). Ultrathin sections incubated with

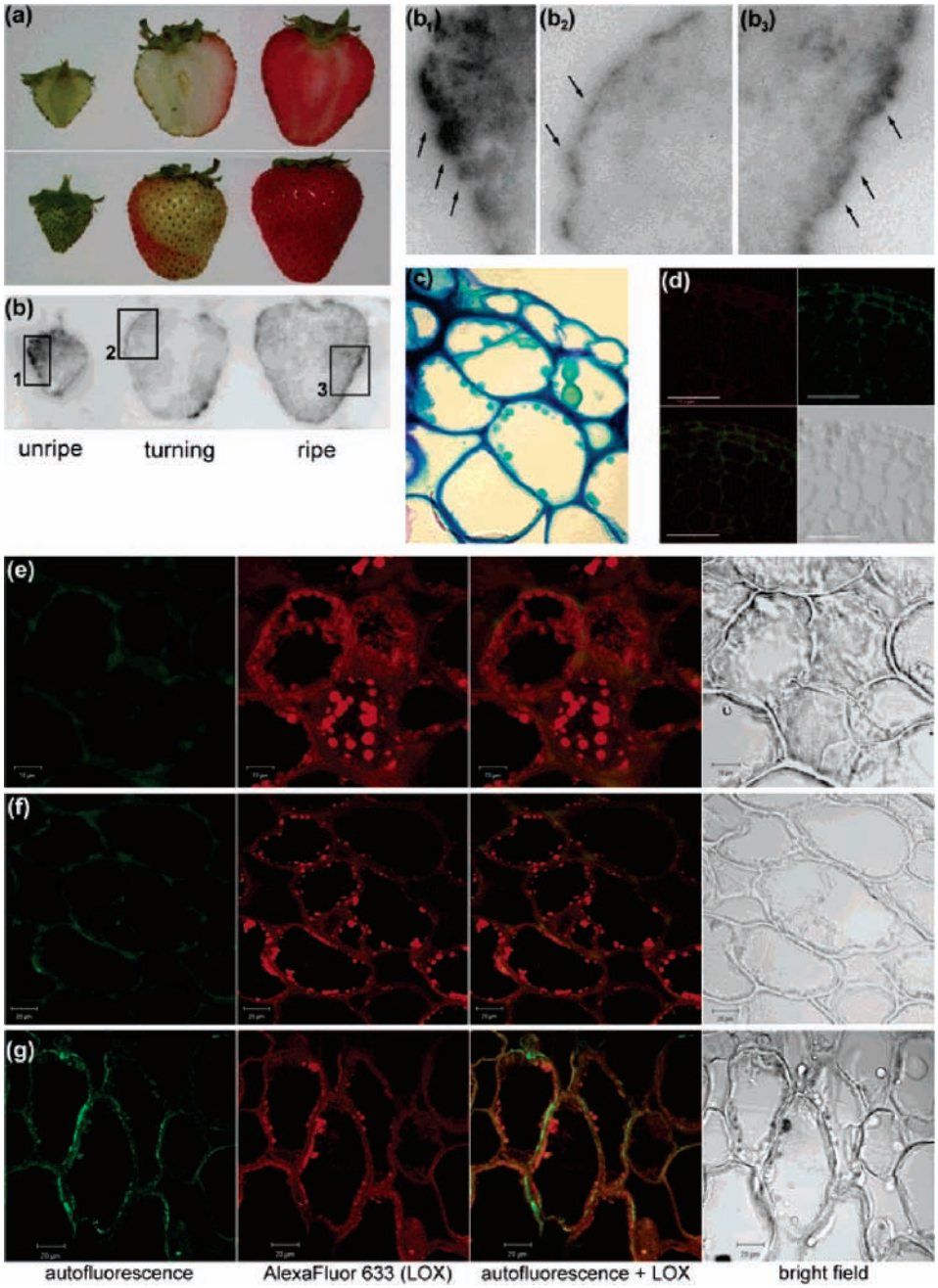

Figure 5. View of strawberry fruit at different stages of ripening at CLSM and light microscopy. (**a**) Confocal image of sagittal sections of strawberry receptacle; (**b**) light micrograph of tissue printing of a fruit section blotted on nitrocellulose membrane and immunostained by anti-LOX antibodies; b_1–b_3, enlargements of the squares in part **b**: an immunoreaction in unripe (b_1), turning (b_2), and ripe (b_3) fruit was observed. (**c**) Toluidine blue-stained section of unripe receptacle showing epidermis and small spherical structures (lipid–protein globules) lying close to the cell wall in the subepidermal parenchyma cells. (**d**) Confocal images of the control treated without anti-LOX antibodies. (**e**–**g**) Confocal fluorescent images of immunolabeled parenchyma cells of (**e**) unripe, (**f**) turning, and (**g**) ripe receptacles. A strongly labeled endomembrane system and lipid–protein globules are detectable. Each image is the overlapping of 10–14 0.7 μm optical sections (*z*-axis) and shows the autofluorescence emission (green, first column), the Alexa Fluor 633 immunolabeled tissues (red, second column), and the matches of autofluorescence and AlexaFluor emissions (green-red, third column). Bright field confocal images were simultaneously collected by photomultiplicator and are represented as gray scale images on the last column.

preimmune serum as the control did not show any specific labeling (**Figure 6d**).

DISCUSSION

The present study suggests that LOX activity is involved in the maturation process of strawberry fruits and is implicated in the lipid metabolism and in the biosynthesis of some derived volatile products during ripening.

The specific activity of LOX in ripening strawberry was high at the unripe and turning stages but significantly decreased in ripe fruits. This decrease in LOX activity was observed in all of the subcellular compartments considered: microsomes, soluble, and lipid body-enriched fractions. Western blots of strawberry proteins showed that a number of forms were present, corresponding to at least two mobility groups. The bands detected by anti-LOX (raised against cucumber LOX) (*32*) after

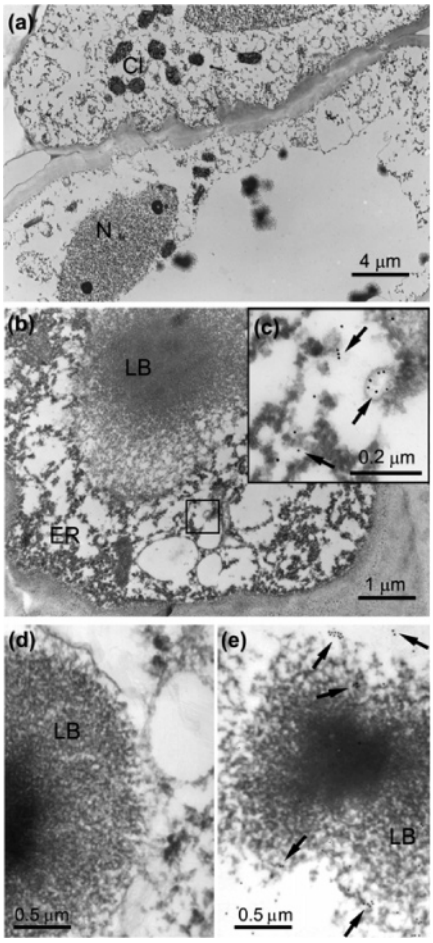

Figure 6. Micrographs of LOX immunolocalization in parenchyma tissue of strawberry fruits. (**a**) General view of two parenchyma cells in unripe strawberry where the membrane aggregates (LB) are detectable. In the bulk of the cytoplasm nuclei (N), chloroplasts (Cl), and endomembrane system are recognizable. (**b**) Section of a parenchyma cell, treated with anti-LOX antibody and secondary anti-rabbit antibody, 10 nm gold conjugated, showing a globular lipid–proteinlike structure (LB). The lipid–proteinlike structures are electron-dense structures, round in shape with a dense core. (**c**) Enlarged view of square in part **b**: lipid–proteinlike structures seem to be interconnected each other and labeled at their outer face by clusters of gold particles (arrows). Labeled gold particles are detectable at the less condensed surface (arrows) while the dense body is unlabeled. (**d**) High magnification of a globular body incubated with primary antiserum alone as control. No labeling of the structures is evident. (**e**) Enlargement of a globular body (LB) incubated with anti-LOX and gold-labeled secondary antibodies: The structure seems to be an irregular aggregate of electron-dense material (presumably lipid–protein aggregates); gold particles are associated to LOX proteins, mainly enriching the profiles of membranous structures (endoplasmic reticulum?, ER) at the outer part of the lipid–protein aggregates; the electron dense core is unlabeled.

one-dimensional gel electrophoresis were of a size consistent with LOXs reported by other authors (*1*). Analysis of the immunoreactive spots present in 2DE blotting confirmed the presence at all ripening stages of different isoforms of LOX enzymes with different molecular masses (80−100 kDa) and isoelectric points (pI) ranging from pI 4.4 to pI 6.5. The 2D analysis showed more than ten immunoreactive spots, some of which were present throughout ripening, while others only appeared at specific stages. In unripe fruits, neutral−acidic immunoreactive spots were prevalent, while a dominance of almost neutral pI spots were evident at the turning and the ripe stages. Droillard et al. (*34*). found acidic LOX isoforms with a pI of between 4 and 5 in membrane-bound enzymes and in the soluble fraction of tomato pericarp. Ripening-related LOXs were also reported in tomato fruits (*35*). These observations together with our finding of 9- and 13-LOX activity, 2DE detached LOX forms, and the fact that cell compartments can have different pH values, could suggest the presence of various LOX forms with different cell localization during strawberry ripening.

Analysis of different subcellular fractions in ripening fruits indicated a relevant LOX activity associated to the LBF that was highest when assayed either with TLA or TLNA, especially at the early ripening stage. This activity may be due to a particular isoform of LOX able to bind target membranes such as that described by May et al. (*36*). These data are in agreement with previous reports, describing enzymes capable of oxygenating the esterified unsaturated fatty acid located in the lipid bodies (*2*) and biomembranes (*37*, *34*), via a LOX-like mechanism. The results also underlined a microsome associate LOX activity, able to oxygenate both free and complex unsaturated fatty acids. The membrane-associated activity decrease during ripening may be due to two simultaneous events: membrane degradation and reduced substrate. Previous studies have demonstrated that plant 13-LOXs oxygenate polyenoic fatty acids esterified within phospholipids or triacylglycerols (*38*, *20*), and the presence of different 13-LOX forms involved in the oxygenation of complex substrates, such as TLA, has been suggested (*2*). Strong arguments were also produced for in vivo LOX-mediated oxygenation of polyunsaturated fatty acid residues in complex storage lipids (*39*).

Concerning the LOX activity in the soluble fraction during ripening, a decrease was observed when the assay was performed in the presence of LA and LNA, but no specific behavior was shown when esterified fatty acids were used as substrates. It is likely that soluble LOX activity belongs to a distinct family or could be a LOX form transiently associated with various biological membranes or could represent a surplus of organelle-bonded enzymes when their intracellular level increases.

The observation that LOXs present in strawberry fruits are able to oxygenate esterefied and nonesterefied fatty acids introduces the question as to whether there are different LOX forms, which add oxygen to fatty acids before or after the action of lipases. From the data presented here, it is not possible to specify whether strawberry LOX activity acts directly on triacylglycerols or is mediated by some lipase activity. However, there is some evidence of high lipase activity in unripe strawberry fruits and its drop in ripe fruits (*10*). This result indicates that a lipase present in strawberry fruits could hydrolyze lipids to form nonesterified fatty acids, which are substrates for LOX-derived hydroperoxides, subsequently converted into volatiles C_6 aldehydes through the LOX-HPL pathway. In strawberry tissues, the concentration of hexanal and *trans*-2-hexenal depends either on the varying availability of substrates in the tissues or on the status of the endomembranes and enzyme forms present at the various ripening stages. In light of these observations, it is possible to postulate that many LOX isoenzymes, occurring with temporal and spatial differences, might have a role in strawberry ripening. Although our data suggest the occurrence of a 9-LOX and a HPL metabolizing 9-HPOT in vitro, the very low amount of nonadienal detected in vivo indicated that the 9-LOX plays a minor role in the production of flavor volatile compounds during strawberry fruit ripening and that the 13-LOX could be sufficient for C_6 volatile

compound production. Our data are in agreement with LOX and HPL activities reported in response to wounding (*11*).

Analysis at cellular and subcellular levels revealed the presence of lipid−protein structures, consisting of membrane aggregates each other interconnected, which seem to be intimately joined to membranous structures. These lipid−protein structures appear to be quite different from plant storage lipid bodies, referred to as spherical homogeneous osmiophilic organelles (storage lipids, mostly triacylglycerols, tightly packed) covered with a phospholipid monolayer and extrinsic proteins. The lipid−protein structures, observed in unripe strawberry, seem to be membranous aggregates (ER profiles?), which undergo morphological changes during ripening. The immunolocalization suggests an association between strawberry LOX and lipid−protein bodylike structures. These structures become dense and enlarged in the ripe receptacle, suggesting a likely coalescence of their lipid component. At the turning stage, the lipid−protein structure seems to be the typical lipid body in oilseed plants (*40*) and the LOXs are localized in their outer surface. During the latter stage of fruit ripening, the structure of parenchyma cells of the receptacle disintegrates completely, releasing the coalesced lipid bodies along the large vacuole, where LOX proteins can be localized. Similar morphological changes in cells of oleaginous fruits were described by Murphy (*41*). In Carnation petals, similar lipid−protein particles were described as enriched C_6 aldehydes and alcohols (*27*).

Although it is not possible to distinguish the different LOX isoenzymes by immunolocalization, the data reported here, coupled with the results on LOX activity in the different subcellular compartments and the Western blot results, allow us to postulate the presence of different LOX isoenzymes with different physiological roles. The presence of 9- and 13-LOX activity in total enzymatic extracts and/or an additional 9-LOX activity present at the unripe and turning stage, could support the occurrence of heterogeneous LOXs in ripening strawberry. The structural modification of lipid−protein globules, together with the spatial localization of LOX, indicates programmed organelle degradation, through a mobilization of membrane lipids. As a consequence, the decrease in LOX proteins and activity during ripening could be related to the structural modifications of the endomembrane system and lipid−protein particles. These results together with the findings of Hudak and Thompson (*27*) on lipid−protein particle-enriched LOX pathway-derived C_6 aldehydes could suggest, for some strawberry LOX, a role in membrane lipid metabolism and C_6 volatile biosynthesis.

In conclusion, some LOX forms may have specific locations in different cell compartments of strawberry fruits and their activity is temporally differentiated. The significance of LOX activity remains unclear, at present; although the production of C_6 aldehydes indicates that a branch of the LOX pathway including HPL is active in ripening strawberry. Further biochemical and molecular experiments are in progress in our laboratory to better characterize the molecular features of strawberry LOXs, their activity, and their product specificity in both receptacles and achenes during ripening.

ABBREVIATIONS USED

LOX, lipoxygenase; HPL, hydroperoxide lyase; LA, linoleic acid; LNA, linolenic acid; MLA, linoleic acid methyl ester; MLNA, linolenic acid methyl ester; TLA, trilinolein; TLNA, trilinolenin; LBF, lipid bodies enriched fraction; SF, soluble-enriched fraction; MF, microsomal-enriched fraction; ER, endoplasmic reticulum; GC-MS, gas chromatography−mass spectrometry; HPO, hydroperoxy fatty acids; 9-,13-HPOD, 9-,-13-hydroperoxy octadecadienoic acids; 9-,13-HPOT, 9-,13-hydroperoxy octadecatrienoic acids; pI, isoelectric point; 9-,-13-HODE, 9-,13-hydroxy octadecadienoic acids; 9-,13-HPTE, 9-,13-hydroxy octadecatrienoic acids; PAGE, polyacrylamide gel electrophoresis; CLSM, confocal laser scanning microscopy; 2DE, bidimensional electrophoresis.

ACKNOWLEDGMENT

We acknowledge Dr. Amedeo Conti for the bidimensional separation of proteins, Prof. Helmut Kindl for critically reviewing the manuscript and for kind gift of the anti-LOX antibody, and Dr. A. Santino and L. D'Amico for helping in HPLC analyses.

LITERATURE CITED

(1) Siedow, J. N. Plant lipoxygenases: Structure and function. *Plant Physiol. Mol. Biol.* **1991**, 145−188.
(2) Feussner, I.; Wasternack, C. The lipoxygenase pathway. *Ann. Rev. Plant Biol.* **2002**, *53*, 275−297.
(3) Fischer, A. M.; Dubbs, W. E.; Baker, R. A.; Fuller, M. A.; Stephenson, L. C.; Grimes, H. D. Protein dynamics, activity and cellular localization of soybean lipoxygenases indicate distinct functional roles for individual isoforms. *Plant J.* **1999**, *19*, 543−554.
(4) Wang, C.; Croft, K. P.; Jarlfors, U.; Hildebrand, D. F. Subcellular localization studies indicate that lipoxygenases 1 to 6 are not involved in lipid mobilization during soybean germination. *Plant Physiol.* **1999**, *120*, 227−236.
(5) Rangel, M.; Machado, O. L., da Cunha, M.; Jacinto, T. Accumulation of chloroplast-targeted lipoxygenase in passion fruit leaves in response to methyl jasmonate. *Phytochemistry* **2002**, *60*, 619−625.
(6) Hause, B.; Weichert, H.; Hohne, M.; Kindl, H.; Feussner, I. Expression of cucumber lipid-body lipoxygenase in transgenic tobacco: Lipid-body lipoxygenase is correctly targeted to seed lipid bodies. *Planta* **2000**, *210*, 708−714.
(7) Trabanger, T. J.; Franceschi, V. R.; Hildebrand, D. F.; Grimes, H. D. The soybean 94-kilodalton vegetative storage protein is a lipoxygenase that is localized in paravenial mesophyll cell vacuoles. *Plant Cell* **1991**, *3*, 973−987.
(8) Vianello, A.; Braidot, E.; Bassi, G.; Macri, F. Lipoxygenase activity on the plasmalemma of sunflower protoplasts and its modulation. *Biochim. Biophys. Acta* **1995**, *1255*, 57−62.
(9) Blée, E. Impact of phyto-oxylipins in plant defense. *Trends Plant Sci.* **2002**, *7*, 315−322.
(10) Leone, A.; Gerardi, C.; Leo, L.; Laddomada, B.; Conti, A.; Bisson, C.; Valentini, S.; Zacheo, G. Analysis of protein expression and the production of aroma compounds during strawberry ripening. *Acta Hortic.* **2003**, *626*, 367−373.
(11) Myung, K.; Hamilton-Kemp, T. R.; Archibold, D. D. Biosynthesis of *trans*-2-hexanal in response to wounding in strawberry fruit. *J. Agric. Food Chem.* **2006**, *54*, 1442−1448.
(12) Veronico, P.; Giannino, D.; Melillo, M. T.; Leone, A.; Reyes, A.; Kennedy, M.; Bleve-Zacheo, T. A novel lipoxygenase in pea roots: its function in wounding and biotic stress. *Plant Physiol.* **2006**, *141*, 1045−1055.
(13) Pérez, A. G.; Sanz, C.; Olìas, R.; Olìas, J. M. Lipoxygenase and hydroperoxide lyase activities in ripening strawberry fruits. *J. Agric. Food Chem.* **1999**, *47*, 249−253.
(14) Rowan, D. D.; Allen, J. M.; Fielder, S.; Hunt, M. B. Biosynthesis of straight chain ester volatiles in red delicious and granny smith apples using deuterium-labelled precursors. *J. Agric. Food Chem.* **1999**, *47*, 2553−2556.
(15) Salas, J. J.; Sànchez, J.; Ramli, U. S.; Manaf, A. M.; Williams, M.; Harwood, J. L. Biochemistry of lipid metabolism in olive and other oil fruits. *Prog. Lipid Res.* **2000**, *39*, 151−180.

(16) Vancanneyt, G.; Sanz, C.; Farmaki, T.; Paneque, M.; Ortego, F.; Castanera, P.; Sanchez-Serrano, J. J. Hydroperoxide lyase depletion in transgenic potato plants leads to an increase in aphid performance. *Proc. Natl. Acad. Sci.* **2001**, *98*, 8139−8144.
(17) Noordermeer, M. A.; Veldink, G. A.; Vliegenthart, J. F. Fatty acid hydroperoxide lyase: A plant cytochrome p450 enzyme involved in wound healing and pest resistance *Chembiochem* **2001**, *2*, 494−504.
(18) Kausch, K. D.; Handa, A. K. Molecular cloning of a ripening-specific lipoxygenase and its expression during wild-type and mutant tomato fruit development. *Plant Physiol.* **1997**, *113*, 1041−1050.
(19) Cass, B. J.; Schade, F.; Robinson, C. W.; Thompson, J. E.; Legge, R. L. Production of tomato flavour volatiles from a crude enzyme preparation using a hollow-fiber reactor. *Biotechnol. Bioeng.* **2000**, *67*, 372−377.
(20) Matsui, K.; Shibata, Y.; Tateba, H.; Hatanaka, A.; Kajiwara, T. Changes of lipoxygenase and fatty acid hydroperoxide lyase activities in bell pepper fruits during maturation. *Biosci., Biotechnol., Biochem.* **1997**, *6*, 199−201.
(21) Gomi, K.; Yamasaki, Y.; Yamamoto, H.; Akimitsu, K. Characterization of a hydroperoxide lyase gene and effect of C6-volatiles on expression of genes of the oxylipin metabolism in *Citrus. J. Plant Physiol.* **2003**, *160*, 1219−1231.
(22) Pérez, A. G.; Olias, R.; Luaces, P.; Sanz, C. Biosynthesis of strawberry aroma compounds through amino acid metabolism. *J. Agric. Food Chem.* **2002**, *50*, 4037−4042.
(23) Sanz, C.; Olìas, J. M.; Pérez, A. G. Aroma biochemistry of fruits and vegetables. In *Phytochemistry of Fruits and Vegetables*; Tomàs-Barberàn, F. A., Robins, R. J., Eds.; University Press: Oxford, United Kingdom, 1997; pp 125−155.
(24) Azodanlou, R.; Darbellay, C.; Luisier, J. L.; Villettaz, J. C.; Amado, R. Quality assessment of strawberries (Fragaria species). *J. Agric. Food Chem.* **2003**, *51*, 715−721.
(25) Aharoni, A.; O'Connell, A. P. Gene expression analysis of strawberry achene and receptacle maturation using DNA microarrays. *J. Exp. Bot.* **2002**, *53*, 2073−2087.
(26) Thompson, J. E.; Froese, C. D.; Madey, E.; Smith, M. D.; Hong, Y. Lipid metabolism during plant senescence. *Prog. Lipid Res.* **1998**, *37*, 119−141.
(27) Hudak, K. A.; Thompson, J. E. Subcellular localization of secondary lipid metabolites including fragrance volatiles in carnation petals. *Plant Physiol.* **1997**, *114*, 705−713.
(28) Bradford, M. M. A rapid and sensitive method for the quantitation of microgram quantities of protein utilizing the principle of protein-dye binding. *Anal. Biochem.* **1976**, *72*, 248−254.
(29) Axelrod, B.; Cheesbrough, T. M.; Laakso, S. Lipoxygenase from soybeans. *Methods Enzymol.* **1981**, *71*, 441−451.
(30) Santino, A.; De Paolis, A.; Gallo, A.; Quarta, A.; Casey, R.; Mita, G. Biochemical and molecular characterization of hazelnut (*Corylus avellana*) seed lipoxygenases. *Eur. J. Biochem.* **2003**, *270*, 4365−4375.
(31) Hsu, A. F.; Shen, S.; Wu, E.; Foglia, T. A. Characterization of soybean lipoxygenase immobilized in cross-linked phyllosilicates. *Biotechnol. Appl. Biochem.* **1998**, *28*, 55−59.
(32) Feussner, I.; Kindl, H. A lipoxygenase is the main lipid body protein in cucumber and soybean cotyledons during the stage of triglyceride mobilization. *FEBS Lett.* **1992**, *298*, 223−225.
(33) Leone, A.; Melillo, M. T.; Bleve-Zacheo, T. Lipoxygenase in pea roots subjected to biotic stress. *Plant Sci.* **2001**, *161*, 703−717.
(34) Droillard, M. J.; Rouet-Mayer, M. A.; Bureau, J. M.; Lauriere, C. Membrane-associated and soluble lipoxygenase isoforms in tomato pericarp (characterization and involvement in membrane alterations). *Plant Physiol.* **1993**, *103*, 1211−1219.
(35) Smith, J. J.; Linforth, R.; Tucker, G. A. Soluble lipoxygenase isoforms from tomato fruit. *Phytochemistry* **1997**, *45*, 453−458.
(36) May, C.; Höhne, M.; Gnau, P.; Schwennesen, K.; Kindl, H. The N-terminal beta-barrel structure of lipid body lipoxygenase mediates its binding to liposomes and lipid bodies. *Eur. J. Biochem.* **2000**, *267*, 1100−1109.
(37) Brash, A. R.; Ingram, C. D.; Harris, T. M. Analysis of a specific oxygenation reaction of soybean lipoxygenase-1 with fatty acids esterified in phospholipids. *Biochemistry* **1987**, *26*, 5465−5471.
(38) Holtman, W. L.; Vredenbregt-Heistek, J. C.; Schmitt, N. F.; Feussner, I. Lipoxygenase-2 oxygenates storage lipids in embryos of germinating barley. *Eur. J. Biochem.* **1997**, *248*, 452−458.
(39) Weichert, H.; Kolbe, A.; Kraus, A.; Wasternack, C.; Feussner, I. Metabolic profiling of oxylipins in germinating cucumber seedlings—Lipoxygenase-dependent degradation of triacylglycerols and biosynthesis of volatile aldehydes. *Planta* **2002**, *215*, 612−619.
(40) Huang, A. H. C. Oil bodies and oleosins in seeds. *Ann. Rev. Plant Physiol. Mol. Biol.* **1992**, *43*, 177−200.
(41) Murphy, D. J. The biogenesis and functions of lipid bodies in animals, plants and microorganisms. *Prog. Lipid Res.* **2001**, *40*, 325−438.

Received for review May 23, 2006. Revised manuscript received July 6, 2006. Accepted July 9, 2006. This work was financially supported by MURST (FISR D.M. 10/5/00 in G.U. 195, 22/8/00).

JF061457G